

# UCLA

## UCLA Previously Published Works

### Title

5-(2-[18 F]Fluoroethyl)-4-Methylthiazole Probe For Positron Emission Tomography Of The Central Nervous System

### Permalink

<https://escholarship.org/uc/item/46k1r1zp>

### Journal

Chemistry of Heterocyclic Compounds, 50(2)

### ISSN

0132-6244

### Authors

Evdokimov, NM  
Flores, G  
Clark, PM  
et al.

### Publication Date

2014-05-01

### DOI

10.1007/s10593-014-1477-4

Peer reviewed

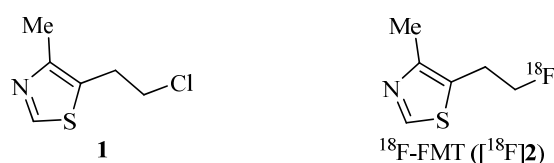
**5-(2-[<sup>18</sup>F]FLUOROETHYL)-4-METHYLTHIAZOLE PROBE  
FOR POSITRON EMISSION TOMOGRAPHY  
OF THE CENTRAL NERVOUS SYSTEM**

**Keywords:** 5-(2-[<sup>18</sup>F]fluoroethyl)-4-methylthiazole, central nervous system, fluorination, imaging, neuroprotection, positron emission tomography, radiolabeling.

Positron emission tomography (PET) is a non-invasive diagnostic method of high clinical utility [1]. Current clinical PET scanning of brain functions rely heavily on two tracers, 2-deoxy-2-[<sup>18</sup>F]fluoro-D-glucose (18F-FDG) [2] and the more selective 3,4-dihydroxy-6-[<sup>18</sup>F]fluoro-L-phenylalanine (18F-FDOPA) [3]. Although it is used to track fundamental sugar metabolism, the FDG probe sometimes lacks selectivity, especially for the imaging of high grade brain tumors after treatment [4]. Better resolution can be achieved with radiolabeled amino acids [5]. Unfortunately, imaging of amino acid metabolism with FDOPA offers indirect conclusions based on the low probe uptake in Parkinson's and Alzheimer's diseases

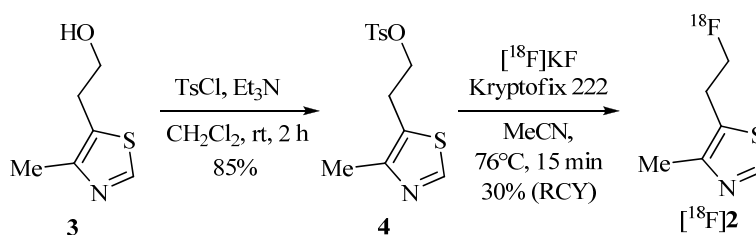
[6]. The emerging interest in *in vivo* real time imaging of memory functioning and age-caused neurodegeneration has been limited due to the small number of existing selective PET tracers. Accordingly, development of new probes which target alternative brain receptors could dramatically advance our understanding of the specific processes occurring within the brain and would potentially offer an alternative avenue in clinical patient diagnosis.

Neuronal excitotoxicity is one of the major mechanisms hypothesized to be involved in the development of neurodegenerative conditions such as Alzheimer's disease [7]. It is characterized by the overstimulation of excitatory glutamate receptors leading to an increased concentration of calcium ions, which trigger several cell-damaging processes, resulting in dysfunction and the death of neurons [8]. Since they display neuroprotection during Alzheimer's disease [9], GABA receptor agonists based on a benzodiazepine core are of particular interest for imaging the adverse effects of neurodegeneration [10]. Selective agonists of GABA receptors have been also shown to exhibit neuroprotective properties in ischemic stroke [11]. In particular, clomethiazole **1** (CMZ, Heminevrin) is a GABA<sub>A</sub> receptor agonist and a prescription sedative and hypnotic drug with pronounced neuroprotective function [12]. However, it was shown to be ineffective in improving the outcome of patients with major ischemic stroke [13].



We envisioned that substitution of the terminal chlorine atom with a radioactive fluorine atom would afford an analog of CMZ, 5-(2-[<sup>18</sup>F]fluoroethyl)-4-methylthiazole (<sup>18</sup>F-FMT) ([<sup>18</sup>F]**2**), which would bind in a similar fashion to a site on the GABA receptor. The non-radioactive 5-(2-fluoroethyl)-4-methylthiazole (FMT) (**2**), which is readily available upon reaction of sulfurol (**3**) with DAST, was previously shown to have bacteriostatic activity against *E. coli* [14]. It was anticipated that use of the <sup>18</sup>F-labeled FMT probe would reveal regions of the central nervous system (CNS) with an overexpression of GABA receptors and would likely image neuronal inhibition *in vivo*.

The synthetic challenges in radiolabeling with the <sup>18</sup>F isotope arise from its short half life – 110 min. Therefore, the radiosynthesis of compound [<sup>18</sup>F]**2** was planned so that the radiolabel would be introduced by a fast S<sub>N</sub>2 reaction. Thus the reaction of the commercially available alcohol **3** with tosyl chloride produced tosylate **4** [15], which in a reaction with <sup>18</sup>F-labelled potassium fluoride afforded the <sup>18</sup>F-probe of compound [<sup>18</sup>F]**2** in one step with both high radio-corrected yield (RCY) and purity.



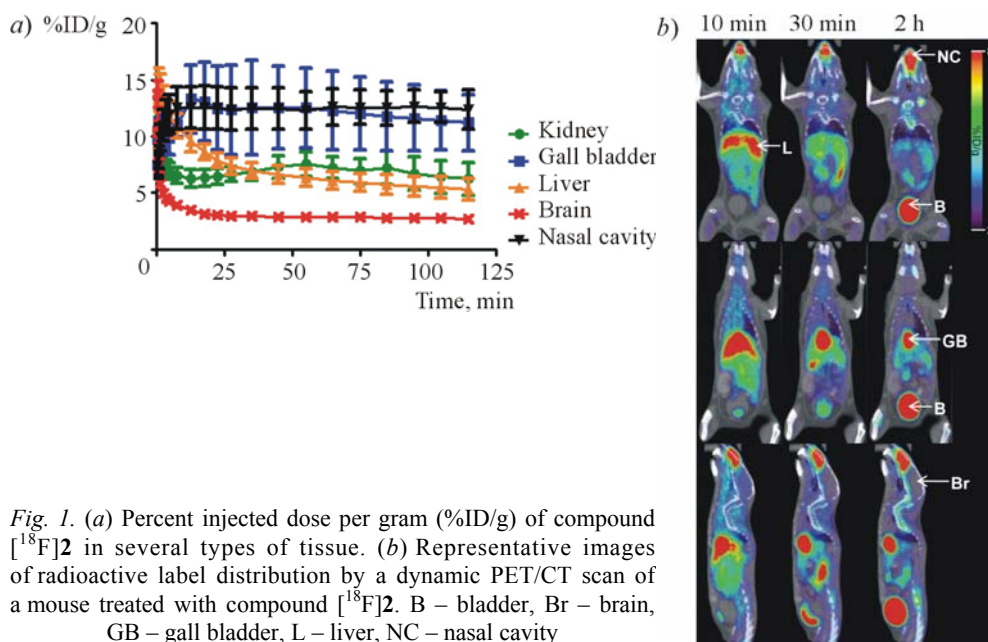


Fig. 1. (a) Percent injected dose per gram (%ID/g) of compound  $[^{18}\text{F}]\mathbf{2}$  in several types of tissue. (b) Representative images of radioactive label distribution by a dynamic PET/CT scan of a mouse treated with compound  $[^{18}\text{F}]\mathbf{2}$ . B – bladder, Br – brain, GB – gall bladder, L – liver, NC – nasal cavity

The  $^{18}\text{F}$ -FMT probe ( $[^{18}\text{F}]\mathbf{2}$ ) thus obtained was subjected to quality control and used for PET scanning of wild type mice. These mice were devoid of tumors or xenografts, and the results of these experiments show the normal biodistribution of the probe. As early as 10 min after injection, strong radioactive accumulation in the liver and nasal cavity was observed. Over the next two hours, the radioactivity continued to accumulate in the nasal cavity and began to accumulate in the bladder and gall bladder (Fig. 1). This latter signal suggests hepatic and renal clearance of the probe.

To determine whether the signal in the nasal cavity represents specific accumulation, we performed a competition experiment between compound  $^{18}\text{F}$ -FMT ( $[^{18}\text{F}]\mathbf{2}$ ) and non-radioactive FMT ( $\mathbf{2}$ ). Mice co-injected with 6.25  $\mu\text{mol}$  of non-radioactive FMT and  $^{18}\text{F}$ -FMT showed significantly lower  $^{18}\text{F}$ -FMT accumulation in the nasal cavity compared to mice co-injected with vehicle and  $^{18}\text{F}$ -FMT (Fig. 2). Alternatively,  $^{18}\text{F}$ -FMT accumulation in the brain was unaffected by co-injection with non-radioactive FMT (Fig. 2). This suggests that  $^{18}\text{F}$ -FMT accumulates in the nasal cavity through a saturable accumulation mechanism.

In conclusion, attempting to selectively image the central nervous system, we have synthesized a new PET probe based on a known thiazole heterocyclic drug clomethiazole. The probe  $^{18}\text{F}$ -FMT did not display a strong and selective signal in the CNS, but we have observed that radioactivity accumulated in the nasal cavity.

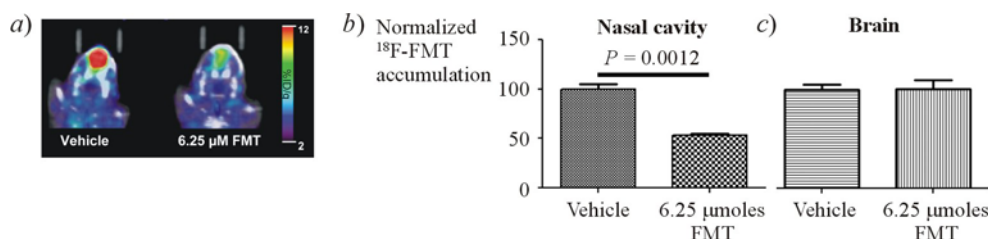


Fig. 2.  $^{18}\text{F}$ -FMT signal in the nasal cavity decreases in the presence of non-radioactive FMT. Quantification of  $^{18}\text{F}$  signal in the nasal cavity (b) and brain (c). Representative images of  $^{18}\text{F}$  signal in the nasal cavity of mice injected with  $^{18}\text{F}$ -FMT and vehicle (a, left) or  $^{18}\text{F}$ -FMT and 6.25  $\mu\text{M}$  non-radioactive FMT (a, right)

Although the probe was shown to be stable in bench stability experiments, a weak signal in the bones suggested some formation of free fluoride *in vivo*. The experiment with non-radioactive FMT showed a diminished accumulation of radioactivity within nasal cavity, suggesting a competitive tissue-specific biodistribution of the probe. The observed signal in the liver and bladder pointed to the hepatic and renal clearance of the probe or its metabolites. Further work on this probe is underway.

Anhydrous solvents, K<sub>2</sub>CO<sub>3</sub>, and 4,7,13,16,21,24-hexaoxa-1,10-diazabicyclo[8.8.8]hexacosane (Kryptofix 222, K222) were purchased from Sigma Aldrich. Solid phase extraction cartridges, silica Sep-Pak WAT020520, and Sep-Pak Plus Alumina N Cartridges WAT 020510 were purchased from Waters Associates. The silica gel cartridge was preconditioned with 10 ml of anhydrous hexane, and the alumina cartridge was preconditioned with 10 ml of water. The reference standard compound **2** was synthesized according to a published protocol [14].

**The radiosynthesis of 5-(2-[<sup>18</sup>F]fluoroethyl)-4-methylthiazole ([<sup>18</sup>F]**2**) and its purification.** No-carrier-added [<sup>18</sup>F]KF was produced in a RDS-111 cyclotron from [<sup>18</sup>O]H<sub>2</sub>O (98% isotopic purity, Rotem, Inc.) on a silver target. An aliquot of aqueous [<sup>18</sup>F]KF (250 μl) was treated with a premixed solution of K<sub>2</sub>CO<sub>3</sub> (1.5 mg) in H<sub>2</sub>O (14 μl) and Kryptofix 222 (10 mg) in anhydrous MeCN (950 μl). The mixture was heated to 120°C under dry nitrogen and dried repeatedly with 4 × 0.5 ml of anhydrous MeCN. In the next step, 16 mg of 2-(4-methylthiazol-5-yl)ethyl 4-methylbenzenesulfonate (**4**) dissolved in anhydrous MeCN (500 μl) was added to the dried <sup>18</sup>F-KF/K222 complex and the reaction mixture was heated to 76°C for 15 min in a sealed vessel. The cooled reaction mixture was loaded onto a silica gel cartridge and the fluorinated product was eluted with anhydrous ethyl acetate (3 ml) into a second reaction vessel. The solvent was then evaporated at 80°C under a flow of dry nitrogen. The resulting dried residue was dissolved in water (500 μl) and passed through an alumina cartridge and eluted with sterile injectable water (4 ml) that was sterilized by filtration through a 0.22 μm filter. The final product was formulated in 10% EtOH in H<sub>2</sub>O.

Analytical HPLC was performed with a WellChrom K-505 HPLC pump (Knauer, Berlin, Germany), analytical phase Luna column (5 μm, 10 × 250 mm, Phenomenex), UV detector (254 nm, WellChrom Spectro-Photometer K-505, Knauer), and gamma radiation detector and counter (B-FC-3300 and B-FC-1000, Bioscan, Inc.). The mobile phase was 50% MeCN in H<sub>2</sub>O (flow rate 1 ml/min, retention time 3.5 min). All chromatograms were collected using a GinaStar analog-to-digital converter (Raytest U.S.A., Inc.) and GinaStar software (Raytest U.S.A., Inc.) running on a PC. The radiochemical purity of the probe was shown to be 99%.

**The PET experiment.** Approximately 100 μCi of <sup>18</sup>F-FMT was injected intravenously into the tail vein of anesthetized 8–12 week female C57Bl/6 mice. Each mouse was subject to a 2 h dynamic PET scan on a microPET imager (Inveon, Siemens Medical Solutions U.S.A., Inc.). For the competition experiments, approximately 20 μCi of <sup>18</sup>F-FMT was co-injected intravenously into the tail vein with non-radioactive FMT (6.25 μmol) or vehicle (1.25% DMSO in 1× phosphate buffered saline). After 1 h, each mouse was subject to a 10 min static PET scan on a microPET imager (G4, Sofie Biosciences). Following the PET scans, each mouse was subjected to a 10 min computed tomography (CT) scan on a microCT imager (MicroCAT, Imtek, Inc.). The PET images were reconstructed and co-registered with the CT image [16]. PET/CT images were analyzed and quantified using the AMIDE software [17]. Images are representative of *n* = 3–5 independent experiments.

*N. M. E. was supported by The Phelps Family Foundation. P. M. C. was supported by the California Institute of Regenerative Medicine (Training Grant TG2-01169) and by the UCLA Scholars in Molecular Imaging Program (NCI R25T CA098010).*

## REFERENCES

1. M. E. Phelps, *Proc. Natl. Acad. Sci. U. S. A.*, **97**, 9226 (2000).
2. D. H. S. Silverman, *J. Nucl. Med.*, **45**, 594 (2004).
3. W. Chen, D. H. S. Silverman, S. Delaloye, J. Czernin, N. Kamdar, W. Pope, N. Satyamurthy, C. Schiepers, T. Cloughesy, *J. Nucl. Med.*, **47**, 904 (2006).

4. M. V. Padma, S. Said, M. Jacobs, D. R. Hwang, K. Dunigan, M. Satter, B. Christian, J. Ruppert, T. Bernstein, G. Kraus, J. C. Mantil, *J. Neurooncol.*, **64**, 227 (2003).
5. F. Bénard, J. Romsa, R. Hustinx, *Semin. Nucl. Med.*, **33**, 148 (2003).
6. D. J. Brooks, *J. Nucl. Med.*, **51**, 596 (2010).
7. R. Cacabelos, M. Takeda, B. Winblad, *Int. J. Geriatr. Psychiatry*, **14**, 3 (1999).
8. M. P. Mattson, *Neuromol. Med.*, **3**, 65 (2003).
9. P. R. Louzada, A. C. Paula Lima, D. L. Mendonça-Silva, F. Noël, F. G. De Mello, S. T. Ferreira, *FASEB J.*, **18**, 511 (2004).
10. H. Boecker, A. Weindl, D. J. Brooks, A. O. Ceballos-Baumann, C. Liedtke, M. Miederer, T. Sprenger, K. J. Wagner, I. Miederer, *J. Nucl. Med.*, **51**, 1030 (2010).
11. A. R. Green, A. H. Hainsworth, D. M. Jackson, *Neuropharm.*, **39**, 1483 (2000).
12. J. W. B. Marshall, A. J. Cross, D. M. Jackson, A. R. Green, H. F. Baker, R. M. Ridley, *Brain Res. Bull.*, **52**, 21 (2000).
13. P. Lyden, A. Shuaib, K. Ng, K. Levin, R. P. Atkinson, A. Rajput, L. Wechsler, T. Ashwood, L. Claesson, T. Odergren, E Salazar-Grueso, *Stroke*, **33**, 122 (2002).
14. G. Lowe, B. V. L. Potter, *J. Chem. Soc., Perkin Trans. 1*, 2026 (1980).
15. H. Zhao, F. W. Foss, R. Breslow, *J. Am. Chem. Soc.*, **130**, 12590 (2008).
16. P. L. Chow, D. B. Stout, E. Komisopoulou, A. F. Chatziioannou, *Phys. Med. Biol.*, **51**, 379 (2006).
17. A. M. Loering, S. S. Gambhir, *Mol. Imaging*, **2**, 131 (2003).

**N. M. Evdokimov<sup>1,2\*</sup>, G. Flores<sup>2,4</sup>, P. M. Clark<sup>3</sup>,  
M. E. Phelps<sup>2,4</sup>, O. N. Witte<sup>2,3,5,6</sup>, M. E. Jung<sup>1\*</sup>**

<sup>1</sup> *University of California, Los Angeles,  
Department of Chemistry and Biochemistry,  
607 Charles E. Young Drive East, Box 951569  
Los Angeles CA 90095-1569, U.S.A.  
e-mail: nevdokim@chem.ucla.edu  
e-mail: jung@chem.ucla.edu*

*Received 16.01.2014*

<sup>2</sup> *University of California, Los Angeles,  
Department of Molecular and Medical Pharmacology,  
650 Charles E. Young Dr. South, 23-120 Center for Health Sciences,  
Los Angeles CA 90095-1735, U.S.A.  
e-mail: owenwitte@mednet.ucla.edu  
e-mail: MPhelps@mednet.ucla.edu  
e-mail: GFlores@mednet.ucla.edu*

<sup>3</sup> *University of California, Los Angeles,  
Department of Microbiology, Immunology, and Molecular Genetics,  
609 Charles E. Young Drive East,  
Los Angeles CA 90095-1489, U.S.A.  
e-mail: PClark@mednet.ucla.edu*

<sup>4</sup> *University of California, Los Angeles,  
Crump Institute for Molecular Imaging,  
570 Westwood Plaza, Los Angeles CA 90095, U.S.A.*

<sup>5</sup> *Eli and Edythe Broad Center  
of Regenerative Medicine and Stem Cell Research,  
University of California, Los Angeles,  
Los Angeles CA 90095, U.S.A.*

<sup>6</sup> *Howard Hughes Medical Institute,  
David Geffen School of Medicine,  
University of California, Los Angeles,  
Los Angeles CA 9009, U.S.A.*

XFC. – 2014. – №. 2. – C. 330